Journal of Applied Physics

Mixing and electronic entropy contributions to thermal energy storage in low melting point alloys

Cite as: J. Appl. Phys. **122**, 025105 (2017); https://doi.org/10.1063/1.4990984
Submitted: 23 April 2017 . Accepted: 17 June 2017 . Published Online: 11 July 2017

Patrick J. Shamberger, Yasushi Mizuno, and Anjana A. Talapatra

Mixing and electronic entropy contributions to thermal energy storage in low melting point alloys

Patrick J. Shamberger,[a] Yasushi Mizuno, and Anjana A. Talapatra
Department of Materials Science and Engineering, Texas A&M University, College Station, Texas 77843, USA

(Received 23 April 2017; accepted 17 June 2017; published online 11 July 2017)

Melting of crystalline solids is associated with an increase in entropy due to an increase in configurational, rotational, and other degrees of freedom of a system. However, the magnitude of chemical mixing and electronic degrees of freedom, two significant contributions to the entropy of fusion, remain poorly constrained, even in simple 2 and 3 component systems. Here, we present experimentally measured entropies of fusion in the Sn-Pb-Bi and In-Sn-Bi ternary systems, and decouple mixing and electronic contributions. We demonstrate that electronic effects remain the dominant contribution to the entropy of fusion in multi-component post-transition metal and metalloid systems, and that excess entropy of mixing terms can be equal in magnitude to ideal mixing terms, causing regular solution approximations to be inadequate in the general case. Finally, we explore binary eutectic systems using mature thermodynamic databases, identifying eutectics containing at least one semiconducting intermetallic phase as promising candidates to exceed the entropy of fusion of monatomic endmembers, while simultaneously maintaining low melting points. These results have significant implications for engineering high-thermal conductivity metallic phase change materials to store thermal energy. *Published by AIP Publishing.*
[http://dx.doi.org/10.1063/1.4990984]

I. INTRODUCTION

The entropy of fusion of substances has long been a subject of interest in both the theoretical and applied physics communities.[1–12] From a fundamental perspective, the entropy of fusion, $\Delta_{fus}S$, is a quantitative measure of changes in order between solid and liquid states. Therefore, $\Delta_{fus}S$ provides insight into the existence and magnitude of different ordering mechanisms in both of those states. Of more practical interest, $\Delta_{fus}S$ plays a pivotal role in the use of melting as a vector to store thermal energy. At the melting temperature of a substance, the specific heat of fusion, $\Delta_{fus}H_w$, is given by

$$\Delta_{fus}H_w = T_{fus} \times \Delta_{fus}S_\mu/M, \tag{1}$$

where T_{fus} is the melting temperature, $\Delta_{fus}S_\mu$ is the molar entropy of fusion, and M is the molar mass of the substance. Thus, for a material to express a large $\Delta_{fus}H_w$ at some temperature T_{fus}, it is beneficial to introduce additional entropic mechanisms in the melting process which may increase $\Delta_{fus}S_\mu$.

The entropy of fusion of simple substances is composed of contributions from multiple independent mechanisms

$$\Delta_{fus}S = \Delta_{config}S + \Delta_{vol}S + \Delta_{rot}S + \Delta_{mix}S + \Delta_{elec}S + \cdots. \tag{2}$$

This expression includes configurational and volume expansion (or contraction) terms ($\Delta_{config}S$, $\Delta_{vol}S$) present in all substances, which vary with the crystal structure of the substance melting.[3–5] In the case of molecular solids, melting also introduces rotational degrees of freedom of a molecule (e.g., diatomic halogen molecules)[6,7] or rotational degrees of freedom along the backbone of a long chain molecule (e.g., paraffins)[8,9] which do not exist in the crystalline solid state ($\Delta_{rot}S$). These initial terms are fairly well understood in simple substances and offer little additional latitude for enhancement. In addition, multi-component systems can express different atomic ordering between components in both solid and liquid states, the extent of which depends on chemical interactions in the system ($\Delta_{mix}S$).[10] Finally, anomalously large $\Delta_{fus}S$ are observed in semiconducting systems and are attributed to delocalization of covalently bound electrons in the liquid, leading to an increase in the electronic entropy of the system ($\Delta_{elec}S$).[11,12] The availability and magnitude of these latter two mechanisms in real multicomponent systems is presently not well constrained.

The capture and storage of thermal energy during melting of a phase change material (PCM) is a critical component of many advanced thermal management (TM) systems. PCMs allow for thermal buffering of devices and systems, absorbing transient heat fluxes, thereby reducing instantaneous demands on heat rejection systems during the period of maximum heat production. For this reason, PCMs have been integrated across a wide range of TM applications including automotive, aerospace, building, and electronics systems.[13–16] The primary material properties of interest for a PCM are the magnitude of its latent heat of fusion, $\Delta_{fus}H$, which governs the total energy stored in a fixed quantity of material, and the temperature at which that material melts, T_{fus}. While in many cases, PCMs are selected from known materials with T_{fus} within a given range and with a favorable $\Delta_{fus}H$, this approach offers no

[a]E-mail: patrick.shamberger@tamu.edu. Tel.: 979-458-1086. Fax: 979-862-6835.

guidance for the development of new, high energy-density PCMs to meet demanding TM challenges. In general, identifying chemical mechanisms to increase $\Delta_{fus}H$, at a particular T_{fus}, remains an open challenge.

In applications that demand very short response times, including TM of electronic components, TM is limited by a PCM's ability to rapidly absorb heat.[15,17–19] This property of a PCM is approximated by a materials-dependent cooling figure of merit, FOM_q, which was derived analytically from heat flux cooling power across a constant-temperature boundary condition,[20] and is also related to temperature deviations at a boundary for constant heat flux boundary condition[21] for simple geometry problems. In general, when the ratio of sensible heat to latent heat terms is small (i.e., when the Stefan number is small) $FOM_q \sim \sqrt{k^L \times \Delta_{fus}H_v}$, where k^L is the thermal conductivity of the liquid, and $\Delta_{fus}H_v$ is the volumetric enthalpy of fusion.[20,21] Unfortunately, k^L and, in some cases, $\Delta_{fus}H_v$ of common PCMs (paraffins, salt hydrates, and inorganic salts) tend to be relatively low, which limits their capacity to rapidly absorb heat. To date, efforts to develop high cooling power PCMs have focused primarily on developing composites consisting of a PCM phase coupled with a high thermal conductivity filler (fibers, foam, particles, etc.).[22–24] While these approaches have enabled minor improvements in thermal conductivity, they also tend to be susceptible to separation of fillers over large number of cycles, as well as to damage of foams due repeated volumetric changes associated with melting and solidification.

In direct contrast, metals and alloys represent a relatively unexplored class of PCMs with large intrinsic thermal conductivities due to large concentrations of free electrons in the liquid.[19,25–29] While many metals (transition metals, noble metals, and rare earth metals) melt substantially above room temperature, a family of post-transition metals (or poor metals), long of interest for their properties as solders, spans a range of melting temperatures appropriate for TM of electronic components (from $<25\,^{\circ}C$ to $>200\,^{\circ}C$). Thus, these low melting point alloys may serve a role in TM of transient pulsed electronics.[15,30] Despite these advantages, known low-melting point metals and alloys generally have small specific enthalpies of fusion, $\Delta_{fus}H$, due to the large density of these materials. Thus, there is a strong motivation to seek out new alloy PCMs which simultaneously couple large FOM_q and relatively large $\Delta_{fus}H_w$.

The goal of this particular study was to investigate the capacity of two potential vectors for enhancing thermal storage capacity of low melting point alloys: (1) entropy of mixing contributions, $\Delta_{mix}S$, and (2) electronic entropy contributions, $\Delta_{elec}S$. To achieve this goal, we investigated two ternary low-melting point alloy systems (Sn-Pb-Bi and In-Sn-Bi), which express contributions from both of these entropic vectors. We experimentally measured $\Delta_{fus}H$, T_{fus}, and T_{cr} (crystallization temperatures) in a number of alloys and compounds in these systems. From these observed values, we calculate $\Delta_{fus}S_\mu$ and evaluate mixing and electronic contributions, including the role of non-ideal mixing effects. We place constraints on the relative contributions of the two effects and suggest areas of interest for further PCM alloy development. Finally, we exploit mature thermodynamic databases to identify other large $\Delta_{fus}S_\mu$ binary alloys in the broader family of post-transition metals and metalloids.

II. METHODS

Pure bismuth was obtained from Sigma Aldrich, pure lead and tin were obtained from Alfa Aesar, and pure indium, as well as a series of Sn-Pb-Bi and In-Sn-Bi alloys, was provided by Indium Corporation.[31] All metals and alloys in this study were of high purity (mass fraction, $w > 0.999$, metals basis) and were used as-received. Metals and alloys incorporated in this study are illustrated in Table I.[32,33]

Multiple samples of (10 to 15 mg) of each metal or alloy were prepared for the determination of $\Delta_{fus}H$, T_{fus}, and T_{cr}. All samples were enclosed in T-zero aluminum pans with standard lids (TA Instruments), allowing gas equilibration during experiments. Sample and sample pan/lid masses were measured independently on an Intell-Lab PXC-200 digital balance and are the average of at least five independent measurements for each sample; predicted mass uncertainty $u_r(m)$ based on repeated measurement is ± 0.2 mg at 95% confidence interval.

A TA Instruments Q2000 differential scanning calorimeter (DSC) was used to determine T_{fus}, T_{cr}, and $\Delta_{fus}H$. The calorimeter was calibrated with a pure indium standard ($w > 0.999$) supplied by TA Instrument, using reference values of $\Delta_{fus}H = 28.662\,J\cdot g^{-1}$ and $T_{fus} = 429.75\,K$.[34] Predicted relative uncertainties for individual measurements, based on repeated analysis of indium standards, are $u_r(T_{fus}) = \pm 0.0004$ and $u_r(\Delta_{fus}H) = \pm 0.025$ at a 95% confidence interval. The calibration was verified by determining $\Delta_{fus}H$ and T_{fus} of high purity ($w > 0.999$) bismuth, lead, tin, and indium. Deviations between reported sample averages and reference values, $\delta = (X_{obs} - X_{ref})/X_{ref}$, are within ± 0.0003 and ± 0.02 for T_{fus} and $\Delta_{fus}H$, respectively.[34–36]

Three separate samples underwent three heating and cooling cycles each at a rate of $10\,K\cdot min^{-1}$ over the temperature range: $T = T_{fus} \pm 50\,K$ under a continuous nitrogen flow of $50\,cm^3\cdot min^{-1}$. Reported values for T_{fus} and $\Delta_{fus}H$ are the averages of second and third cycles (excluding the first melting cycle) of all three samples. Following standard DSC techniques, the onset of the melting peak was reported as T_{fus}, defined by the intercept of a linear baseline with the tangent to the melting curve with the maximum slope. Undercooling, ΔT, was calculated as $\Delta T = T_{fus} - T_{cr}$, where T_{cr} was defined as the onset of crystallization, which is marked by an abrupt exothermic event. $\Delta_{fus}H$ was calculated by integration of the area between the curve and the baseline within the temperature range: $T = T_{fus} \pm 15\,K$.

To calculate the volumetric properties, solid densities are calculated at $T = 298\,K$ for each alloy from reported room-temperature densities of elemental solids and intermetallic compounds, assuming that the solid is composed of solid phases calculated by the lever rule[37–44]

$$\rho^{sol} = \left(\sum\nolimits_{\phi} x^{\phi} M^{\phi}\right) \Big/ \left(\sum\nolimits_{\phi} (x^{\phi} M^{\phi})/\rho^{\phi}\right), \qquad (3)$$

TABLE I. Alloy composition.

	Reaction	ID	Indalloy #	x_{In}	x_{Sn}	x_{Pb}	x_{Bi}	$w_{Impurity}$ [a]		Source
								Total	Major impurities[b]	
In	$L \Longleftrightarrow In$	In	4	>0.9999	…	…	…	1.39×10^{-5}		Indium Corp.
Sn	$L \Longleftrightarrow \beta Sn$	Sn	128	…	>0.9999	…	…			Alfa Aesar
Pb	$L \Longleftrightarrow Pb$	Pb	…	…	…	>0.9999	…			Alfa Aesar
Bi	$L \Longleftrightarrow Bi$	Bi	148	…	…	…	>0.9999			Sigma Aldrich
Sn-Pb-Bi system:[c]										
63Sn-37Pb	$L \Longleftrightarrow Pb + \beta Sn$	e_1	106		0.748	0.252	…	28.2×10^{-5}	Ag: 2.6×10^{-5}, As: 7.1×10^{-5}, Cu: 2.9×10^{-5}, Fe: 2.0×10^{-5}, In: 4.0×10^{-5}, Sb: 4.8×10^{-5}	Indium Corp.
42Sn-58Bi	$L \Longleftrightarrow Bi + \beta Sn$	e_2	281		0.555	…	0.445	15.6×10^{-5}	Ag: 2.4×10^{-5}, In: 2.6×10^{-5}, Pb: 6.2×10^{-5}, Sb: 3.4×10^{-5}	Indium Corp.
44.5Pb-55.5Bi	$L \Longleftrightarrow Bi + \beta$	e_3	255		…	0.452	0.548	1.0×10^{-5}		Indium Corp.
15.5Sn-32Pb-52.5Bi	$L \Longleftrightarrow Bi + \beta Sn + X$	E_1	38		0.244	0.288	0.468	6.7×10^{-5}	Ag: 2.2×10^{-5}, Cu: 2.1×10^{-5}, Sb: 1.8×10^{-5}	Indium Corp.
41Sn-1Pb-58Bi		1	75		0.549	0.010	0.440	9.2×10^{-5}	Ag: 2.2×10^{-5}, Sb: 5.1×10^{-5}	Indium Corp.
34Sn-20Pb-46Bi		2	42		0.474	0.157	0.369	7.5×10^{-5}	Ag: 1.3×10^{-5}, In: 2.1×10^{-5}, Sb: 2.6×10^{-5}	Indium Corp.
22Sn-28Pb-50Bi		3	40		0.332	0.245	0.423	13×10^{-5}	Ag: 2.5×10^{-5}, In: 5.7×10^{-5}, Sb: 3.3×10^{-5}	Indium Corp.
18Sn-30Pb-52Bi		4	39		0.279	0.262	0.459	2.6×10^{-5}	Ag: 1.4×10^{-5}	Indium Corp.
In-Sn-Bi system:[c]										
35In-65Bi (*InBi*)	$L \Longleftrightarrow InBi$	InBi	…	0.500	…		0.500			[d]
52In-48Bi (In_2Bi)	$L \Longleftrightarrow In_2Bi$	In_2Bi	…	0.667	…		0.333			[d]
52In-48Sn	$L \Longleftrightarrow \beta + \gamma$	e_1	1E	0.524	0.476		…	4.1×10^{-5}	As: 1.4×10^{-5}, Pb: 1.2×10^{-5}	Indium Corp.
42Sn-58Bi	$L \Longleftrightarrow Bi + \beta Sn$	e_2	281	…	0.555		0.445	15.6×10^{-5}	Ag: 2.4×10^{-5}, In: 2.6×10^{-5}, Pb: 6.2×10^{-5}, Sb: 3.4×10^{-5}	Indium Corp.
33In-67Bi	$L \Longleftrightarrow Bi + InBi$	e_3	53	0.471	…		0.529	17.1×10^{-5}	Sn: 17.1×10^{-5}	Indium Corp.
66In-34Bi	$L \Longleftrightarrow In_2Bi + \beta$	e_5	162	0.780	…		0.220	1.6×10^{-5}		Indium Corp.
30In-16Sn-54Bi	$L \Longleftrightarrow Bi + InBi + \gamma$	E_1	27	0.390	0.213		0.397	7.0×10^{-5}	As: 1.3×10^{-5}, Pb: 3.5×10^{-5}, Sb: 2.0×10^{-5}	Indium Corp.
26In-17Sn-57Bi	$L \Longleftrightarrow Bi + InBi + \gamma$	E_1* [e]	174	0.355	0.220		0.425	11.0×10^{-5}	Ag: 2.2×10^{-5}, Pb: 8.3×10^{-5}	Indium Corp.
50.5In-16.5Sn-33Bi [f]	$L \Longleftrightarrow In_2Bi + \beta + \gamma$	E_2	19	0.595	0.191		0.215	9.3×10^{-5}	As: 2.2×10^{-5}, Pb: 5.8×10^{-5}, Sb: 1.3×10^{-5}	Indium Corp.

[a]Weight uncertainty estimated at $w \pm 0.0001$, as determined by ICP, reported by provider.
[b]Impurities greater than 1.0×10^{-5} impurity are reported.
[c]Alloy name refers to composition in wt. %.
[d]Synthesized in this study from pure metals described earlier.
[e]E_1* designates eutectic composition proposed by Kabassis *et al.*[64]
[f]Field's metal.

where M^{ϕ}, ρ^{ϕ}, and x^{ϕ} are the molar mass, density, and the molar fraction of phase ϕ in the multi-phase solid. This approximation does not take into account the effects of solid-solutions. Despite this simplification, calculated solid densities are within 3% for those solid alloys which have been measured directly. Liquid densities are calculated at T_{fus} for each alloy from temperature-dependent densities of elemental liquids[45–47]

$$\rho^{L}_{In}/g\,cm^3 = 7312.5 - 0.6978 \times T/K, \tag{4a}$$

$$\rho^{L}_{Sn}/g\,cm^3 = 7374.7 - 0.6765 \times T/K, \tag{4b}$$

$$\rho^{L}_{Pb}/g\,cm^3 = 11441 - 1.2795 \times T/K, \tag{4c}$$

$$\rho^{L}_{Bi}/g\,cm^3 = 10725 - 1.2200 \times T/K. \tag{4d}$$

Densities are calculated from Vegard's law, which predicts a linear relationship between molar volume and the molar fraction of constituent elements

$$V^{L}_{\mu} = \left(\sum\nolimits_i x_i \sqrt[3]{M_i/\rho^{L}_i}\right)^3, \tag{5a}$$

$$\rho^{L} = \left(\sum\nolimits_i x_i M_i\right) \Big/ \left(\sum\nolimits_i x_i \sqrt[3]{M_i/\rho^{L}_i}\right)^3, \tag{5b}$$

where M_i, ρ^{L}_i, and x_i are the molar mass, liquid density, and the molar fraction of the ith component in the liquid, respectively.[47] V^{L}_{μ} is the molar volume of the liquid, and $V^{L}_{\mu,i} = M_i/\rho^{L}_i$ is the molar volume of the ith component in the liquid. Calculated densities are within 2% for those liquid alloys which have been previously measured experimentally.

The Thermo-Calc[48] Software TC Binary Solutions database v1.1 was used to access the models of the binary systems (Al - X: X = Zn, Ga, Ge, In, Sn, Sb; Zn - X: X = Ga, Ge, In, Sn, Sb, Pb, Bi; Ga - X: X = As, In, Sn, Sb; Ge - X: X = As, Sb; In-X: X = Sn, Sb, Bi; Sn-X: X = Pb, Bi; Sb-X: X = Pb; and Pb- X: X = Bi) and extract the thermodynamic data at the eutectic points. Thermo-Calc, which is based on the CALPHAD approach,[49] relies on using the Redlich-Kister expression to represent the excess Gibbs energies of the solution phases in the binary models.[50] The lattice stabilities for the pure elements are those standardized as per the SGTE database.[51]

III. THEORY

A. Entropy of mixing

Mixing of two or more components in a solution (solid or liquid) increases the entropy of phase ϕ by a quantity $\Delta_{mix}S^{\phi}$, which is due to an increase in configurational disorder in that phase. Thus, the change in entropy resulting from melting of a system composed of one or more solid phases with at least two components is given by

$$\Delta_{fus}S = \left(S^{L} + \Delta_{mix}S^{L}\right) - \sum\nolimits_{\phi} x^{\phi}\left(S^{\phi} + \Delta_{mix}S^{\phi}\right), \tag{6}$$

where $\Delta_{mix}S^{L}$ and $\Delta_{mix}S^{\phi}$ are the entropy of mixing in the liquid and in a solid phase ϕ, respectively. In eutectic solids, chemical components are segregated between two or more solid phases but are recombined during melting into a single homogeneous liquid. This mechanism can, in principle, lead to greater $\Delta_{mix}S$ in the liquid phase compared to the aggregate $\Delta_{mix}S$ in the solid, thereby increasing the entropy of fusion of eutectics.[10]

In the simplified regular solution model, $\Delta_{mix}S$ in any disordered phase (solid or liquid) is given by

$$\Delta_{mix}S_{ideal} = -R\sum\nolimits_i x_i \ln x_i, \tag{7}$$

where R is the ideal gas constant, and x_i is again the molar fraction of the ith component in the solution. $\Delta_{mix}S_{ideal}$ is strictly positive, as disorder always increases in the mixed state. The net contribution of $\Delta_{mix}S$ to $\Delta_{fus}S$ of eutectic solids, consists of $\Delta_{mix}S^{L} - \sum_{\phi} x^{\phi}\Delta_{mix}S^{\phi}$. The maximum $\Delta_{mix}S_{ideal}$ is ln(N)R, where N is the number of components in the system, given by the case where there are equimolar concentrations of components and no solid solution. Extensive solid solution lessens the net contribution of $\Delta_{mix}S$ to $\Delta_{fus}S$. Birchenall and co-authors calculated the net contribution of $\Delta_{mix}S$ to $\Delta_{fus}S$ of eutectic solids, adopting the regular solution model, and accounting for solid-solution in solid phases[10]

$$\begin{aligned}\Delta_{fus}S = {} & x^{eu}_A \frac{\Delta_{fus}H^{\alpha}}{T^{\alpha}_{fus}} + x^{eu}_B \frac{\Delta_{fus}H^{\beta}}{T^{\beta}_{fus}} \\ & - R\left\{\left[x^{eu}_A \ln x^{eu}_A + x^{eu}_B \ln x^{eu}_B\right] - \left(\frac{x^{\beta}_B - x^{eu}_B}{x^{\beta}_B - x^{\alpha}_B}\right)\right. \\ & \times \left[x^{\alpha}_A \ln x^{\alpha}_A + x^{\alpha}_B \ln x^{\alpha}_B\right] - \left(\frac{x^{eu}_B - x^{\alpha}_B}{x^{\beta}_B - x^{\alpha}_B}\right) \\ & \left. \times \left[x^{\beta}_A \ln x^{\beta}_A + x^{\beta}_B \ln x^{\beta}_B\right]\right\}. \end{aligned} \tag{8}$$

Real solutions include excess terms which describe interactions between individual atomic and molecular constituents. Excess entropy, S^{E}, is given by

$$\Delta_{mix}S_{real} = \Delta_{mix}S_{ideal} + S^{E}, \tag{9}$$

where a negative excess entropy of mixing indicates that mixing of two or more components increases ordering in the phase relative to $\Delta_{mix}S_{ideal}$. S^{E} can be sizeable, rivaling ideal terms in magnitude (and offsetting these terms). Given the magnitude of $\Delta_{mix}S_{ideal}$, and the modifying terms ($\Delta_{mix}S$ in solid phases and non-ideal terms), it is feasible for $\Delta_{mix}S$ to increase $\Delta_{fus}S$ on the order of ~(0 to ln[N])R.

B. Electronic entropy

Electronic entropy constitutes degrees of freedom associated with the electronic states of a material. The electronic entropy of a phase is related to the density of states at the Fermi level, n_F, which governs the available configurational states of valence band electrons[52]

$$S_{elec} = \frac{1}{3}\pi^2 k^2_B T n_F. \tag{10}$$

S_{elec} can be assumed to be negligible for insulators, which have $n_F \sim 0$. In contrast, S_{elec} can be significant for metals; transition metals have $S_{elec} \sim 2R$ due to relatively flat d-bands near the Fermi level.[53]

Significant changes in electronic entropy are associated with transitions between insulating and conducting states (localized to delocalized electron densities). As an example, the metal-insulator transition in VO_2, a prototypical correlated oxide, is associated with a 4 to 5 order of magnitude change in electrical conductivity that is explained by a dramatic delocalization of electrons. This transition is accompanied by ΔS $1.5 \pm 0.1\,R$ (given per mole of VO_2),[54,55] which is partitioned into lattice and electronic contributions. While there remains some discussion in the literature, it is hypothesized that $\Delta_{elec}S$ contributes significantly ($\sim$0.45 to $0.9\,R$)[54–56] to the overall ΔS of the transformation. Similarly, fusion of semiconductors can, in some cases, lead to electrically conductive liquids, which could be assumed to have $n_F > 0$. In these cases, there is a significant increase in S_{elec} of the system upon melting, the magnitude of which can be considered to scale with the extent of electronic delocalization during melting behavior. For the semiconducting elements Si, Ge, Te, the magnitude of $\Delta_{elec}S$ is approximately (4 to 5)R which greatly exceeds $\Delta_{config}S$ and $\Delta_{vol}S$ in these systems.[11,12]

IV. RESULTS

A. Melting and crystallization temperatures

In all cases, T_{fus} is within 3 K of previously reported values; in the majority of cases, this discrepancy is <1 K, and the relative difference $\delta = (T_{fus} - T_{fus,ref})/T_{fus,ref} < 0.4\%$ (Table II). Values of T_{fus} for eutectics are significantly depressed relative to pure end-member metals. This eutectic T_{fus} depression ranges from (37 to 145) K with respect to the lower T_{fus} pure metal end-member.

Undercooling, ΔT, varies significantly within the investigated family of alloys. This variation is not systematically dependent on alloy composition, as exemplified by InBi and In_2Bi, which express dramatically different degrees of undercooling despite their compositional similarity (Table II). Rather, as undercooling is the result of nucleation-limited solidification, it reflects the interfacial energy between the liquid and one or more nucleating solid phases. This is strongly dependent on crystal structure of the solid and the nature of the liquid-solid interface, and thus does not generally behave as a monotonic function of alloy composition. As has been reported previously, pure Sn and Bi are strongly susceptible to undercooling, whereas In and Pb solidify readily.[57,58] In addition, InBi, e_3, and E_1 in the In-Sn-Bi system and e_1 and E_1 in the Sn-Pb-Bi system are notable for having

TABLE II. Melting and solidification temperatures.

	ID	T_{fus} (K)[a]				T_{cr} (K)		ΔT (K)[b]	N	$T_{fus,\,ref}$ (K)	References
		Avg	2σ	2σ rel (%)	δ[c] (%)	Avg	2σ				
In	In	429.69	0.05	0.01	−0.01	428.5	0.5	1.2	3	429.75	65
Sn	Sn	505.06	0.20	0.04	0.00	476.3	29.0	28.7	3	505.08	65
Pb	Pb	600.60	0.02	0.00	0.09	596.6	1.3	4.0	3	600.05	65
Bi	Bi	544.70	0.15	0.03	0.03	511.1	9.7	33.6	3	544.55	65
Sn-Pb-Bi system:											
63Sn-37Pb	e_1	455.88	0.03	0.01	−0.03	445.9	2.7	10.0	3	456	31
42Sn-58Bi	e_2	412.76	0.93	0.23	0.43	404.0	4.0	8.8	3	411	31
44.5Pb-55.5Bi	e_3	399.36	0.15	0.04	0.30	391.7	0.2	7.6	3	398.7	31
										398.15	66
15.5Sn-32Pb-52.5Bi	E_1	368.71	0.44	0.12	0.19	353.9	9.9	14.9	3	368	31
41Sn-1Pb-58Bi	1	407.5	0.17	0.04	−0.12	399.8	0.2	7.7	3	408	31
34Sn-20Pb-46Bi	2	369.99	0.51	0.14	0.27	364.1	0.7	5.9	3	369	31
22Sn-28Pb-50Bi	3	368.34	0.51	0.14	0.64	364.0	2.3	4.3	3	366	31
18Sn-30Pb-52Bi	4	369.18	2.09	0.57	0.05	358.1	1.3	11.1	3	369	31
In-Sn-Bi system:											
35In-65Bi (*InBi*)	InBi	383.77	0.17	0.04	0.20	359.6	3.4	24.2	4	383	67
52In-48Bi (*In_2Bi*)	In_2Bi	363.09	0.10	0.03	0.02	360.6	1.6	2.5	3	363	67
52In-48Sn	e_1	391.86	0.02	0.00	0.22	389.6	0.7	2.3	3	391	31
42Sn-58Bi	e_2	412.43	1.00	0.24	0.35	406.8	7.8	5.6	3	411	31
33In-67Bi	e_3	383.19	0.13	0.03	0.31	364.0	6.6	19.2	3	382	31
66In-34Bi	e_5	345.94	0.08	0.02	0.27	341.5	0.9	4.4	3	345	31
30In-16Sn-54Bi	E_1	354.03	0.19	0.05	0.15	343.4	2.9	10.6	3	354	31
										353.5	68
26In-17Sn-57Bi	E_1*	353.10	0.75	0.21	0.31	346.7	3.2	6.4	3	352	31
										352	68
50.5In-16.5Sn-33Bi	E_2	333.85	0.07	0.02	−0.04	330.8	0.4	3.1	3	333	31
										334	68

[a]Temperature uncertainty estimated at $\pm$ 0.1 K, as determined from average deviation of pure metals from reference values.
[b]$\Delta T = (T_{fus} - T_{cr})$.
[c]$\delta = (T_{fus} - T_{fus,\,ref})/T_{fus,\,ref}$.

large degrees of undercooling. It is important to note that quantitative measures of undercooling depend on experimental factors such as sample volume and geometry, cooling ramp rate, container material, ambient vibrations, and other experimental factors. Thus, these values are principally of use for comparison against other materials tested under similar circumstances.

B. Enthalpy of fusion

Specific enthalpy of fusion, $\Delta_{fus}H_w$, was measured by DSC of all metals and alloys in this study; volumetric and molar enthalpies of fusion were calculated from these quantities using the calculated density of the solid at 298 K and of the liquid at T_{fus}, and the molar weight of the alloy (Table III). $\Delta_{fus}H_w$ of Sn-Pb-Bi alloys (20 to 47) $J{\cdot}g^{-1}$, of In-Sn-Bi alloys (20 to 47) $J{\cdot}g^{-1}$, and of pure metals (23 to 60) $J{\cdot}g^{-1}$, are generally low relative to more common PCMs (paraffins, salt hydrates) due principally to the high density of these materials [Fig. 1(a)]. $\Delta_{fus}H$ of Sn and Bi, as well as of alloys containing significant fractions of β-Sn and Bi phases, tend to have larger $\Delta_{fus}H_w$ ($>40\,J{\cdot}g^{-1}$) due to the contribution of $\Delta_{elec}S$ of these phases. Observed $\Delta_{fus}H_w$ in pure metals are within 2% of previously reported data, whereas $\Delta_{fus}H_w$ in alloys are within 6% of previously reported data.

Volumetric $\Delta_{fus}H_v$ generally exceed those of paraffins, which have relatively low densities, and are comparable with volumetric energy density of salt hydrates within this temperature range [Fig. 1(b)], even competing with some of the highest known low-temperature volumetric energy density observed in certain salt hydrates (including lithium nitrate hydrates and potassium fluoride hydrates).[59,60] $\Delta_{fus}H_v$ are generally greater in solids rather than liquids, with the exception of pure Bi, and certain Bi-rich alloys, which experience a contraction upon melting due to strong directional covalent bonding in the solid phase. Again, $\Delta_{fus}H_v$ are greatest in pure Bi and Sn as well as eutectics that contain significant fractions of these phases (e_1, e_2, E_1 in Sn-Pb-Bi system; e_2, e_3, E_1 in In-Sn-Bi system) due to the contribution of $\Delta_{elec}S$ of these phases, and additionally to the lower relative density of Sn.

In a number of alloys, significantly larger $\Delta_{fus}H$ were measured in the first cycle relative to subsequent cycles

TABLE III. Enthalpy and entropy of fusion.

	Desig.	$\Delta H_{fus}/J{\cdot}g^{-1}$					$\Delta H_{fus,\,ref}$ ($J{\cdot}g^{-1}$)	References	$\Delta H_{vol,\,sol}$ ($J{\cdot}cm^{-3}$)	$\Delta H_{vol,\,liq}$ ($J{\cdot}cm^{-3}$)	ΔH_{fus} ($kJ{\cdot}mol\ atom^{-1}$)	ΔS_{fus} ($J{\cdot}K^{-1}{\cdot}mol\ atom^{-1}$)
		Avg	2σ	2σ rel (%)	δ[a] (%)	N			Avg	Avg	Avg	Avg
In	In	28.8	0.8	2.8	0.38	3	28.662	34	209.5	202.0	3.30	7.69
		28.5	0.2	0.8	−0.54	3			207.5	200.2	3.27	7.62
Sn	Sn	60.1	2.5	4.2	−0.61	3	60.48	36	438.2	422.8	7.14	14.13
		60.6	2.5	4.1	0.17	3			441.7	426.1	7.19	14.24
Pb	Pb	23.4	0.1	0.4	1.19	3	23.08	36	264.8	249.2	4.84	8.06
		23.5	1.3	5.4	1.98	3			266.9	251.1	4.88	8.12
Bi	Bi	53.2	1.4	2.6	0.05	3	53.146	35	521.6	534.7	11.11	20.40
		53.9	0.5	1.0	1.35	3			528.4	541.6	11.26	20.67
Sn-Pb-Bi system:												
63Sn-37Pb	e_1	45.6	2.1	4.6	..	3	…		383.0	370.4	6.43	14.10
42Sn-58Bi	e_2	47.3	1.7	3.5	5.6	3	44.8	31	405.9	410.3	7.52	18.21
44.5Pb-55.5Bi	e_3	20.0	0.7	3.4	−4.5	3	20.9	31	212.6	210.4	4.16	10.40
15.5Sn-32Pb-52.5Bi	E_1[b]	34.6	3.0	8.6	…	3	…		340.3	339.8	6.45	17.50
	E_1[c]	19.5	2.4	12.6	…	3	…		191.4	191.2	3.63	9.84
41Sn-1Pb-58Bi	1	45.9	2.2	4.8	…	3	…		395.7	399.7	7.32	17.97
34Sn-20Pb-46Bi	2[b]	30.5	1.6	5.2	…	3	…		276.0	276.0	5.05	13.66
	2[c]	26.4	0.2	0.9	…	3	…		238.8	238.8	4.37	11.82
22Sn-28Pb-50Bi	3[b]	32.6	2.7	8.4	…	3	…		311.6	311.1	5.82	15.81
	3[c]	17.1	1.7	9.9	…	3	…		163.9	163.7	3.06	8.31
18Sn-30Pb-52Bi	4[b]	36.5	2.0	5.5	5.3	3	34.70	31	354.7	354.5	6.70	18.14
	4[c]	22.2	1.9	8.7	…	3	…		215.9	215.8	4.08	11.04
In-Sn-Bi system:												
35In-65Bi (*InBi*)	InBi	45.2	0.6	1.2	…	4	…		402.6	400.9	7.31	19.06
52In-48Bi (*In_2Bi*)	In_2Bi	30.4	0.1	0.4	…	3	…		257.1	253.1	4.44	12.22
52In-48Sn	e_1	24.2	0.6	2.6	−0.1	3	24.26	69	177.5	171.5	2.83	7.21
42Sn-58Bi	e_2	47.3	1.5	3.1	5.6	3	44.8	31	405.9	410.3	7.52	18.23
33In-67Bi	e_3	43.1	0.5	1.0	…	3	…		386.5	386.3	7.09	18.51
66In-34Bi	e_5	20.4	0.4	1.8	…	3	…		164.8	162.0	2.76	7.98
30In-16Sn-54Bi	E_1	38.0	2.2	5.8	…	3	…		326.6	325.4	5.81	16.42
26In-17Sn-57Bi	E_1*	39.8	2.0	5.0	…	3	…		344.7	344.8	6.20	17.55
50.5In-16.5Sn-33Bi	E_2	27.4	0.4	1.3	…	3	…		221.1	217.4	3.71	11.12

[a] $\delta = (\Delta H_{fus} - \Delta H_{fus,\,ref})/\Delta H_{fus,\,ref}$.
[b] First melting cycle.
[c] Subsequent melting cycles.

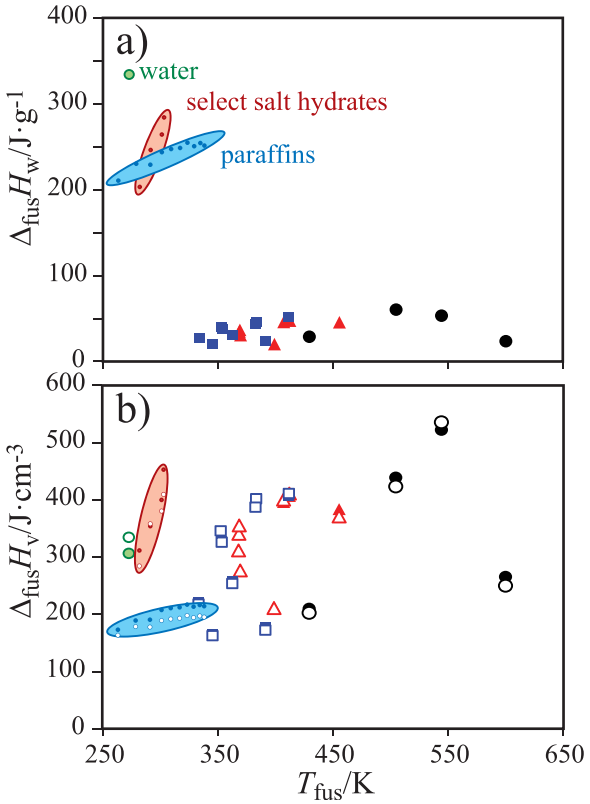

FIG. 1. (a) Specific and (b) volumetric heat of fusion of low melting point metals and alloys in this study. Pure metals are illustrated with black circles, Sn-Pb-Bi alloys with red triangles, and In-Sn-Bi alloys with blue squares. Volumetric heat of fusion of solids is shown with filled symbols, while liquids are shown with empty symbols. Data for water,[70] paraffins,[71,72] and select salt hydrates (lithium nitrate[59] and potassium fluoride hydrates[60]) are included for comparison.

(Table III), which suggests that some volume of material only melted upon the first heating cycle. This observation is generally consistent with materials which melt or solidify incongruently. In such cases, a substance may melt completely on the first cycle, but may compositionally stratify upon solidification due to early solidification of a primary (proeutectic) phase. Such compositionally segregated phases can limit the total extent of melting in future heating cycles, as complete melting would then be diffusionally limited. This feature is observed for points 2, 3, and 4 in the Sn-Pb-Bi system (which are not eutectic points), as well as Indalloy alloy 38, designated here as E1. This result suggests that the tested Indalloy alloy 38 deviates compositionally from a eutectic composition, which would be expected to be an invariant point. Thus, the $\Delta_{fus}H$ observed during the first cycle is representative of melting of the overall alloy (which is typically rapidly quenched from a liquid during synthesis), whereas subsequent cycles cooled relatively slowly during DSC investigation, leading to melting behavior in which only a portion of the sample melts at the originally observed liquidus. This interpretation is consistent with the observation that second (and third) cycles have consistently smaller measured $\Delta_{fus}H$, and that the first melting peak is substantially broader than generally observed, or shows two clearly defined melting peaks (corresponding to both the liquidus temperature for the specific composition, as well as the lower eutectic temperature).

C. Entropy of fusion

Entropies of fusion tend to remain fairly consistent within a given class of materials and are indicative of the magnitude of different mechanisms which operate during the melting of a specific material (e.g., configurational effects, volume expansion effects, rotational degrees of freedom, etc.; Fig. 2). Molar entropies of fusion, $\Delta_{fus}S_\mu$, are calculated from observed enthalpies of fusion according to $\Delta_{fus}S_\mu = \Delta_{fus}H_\mu/T_{fus}$. $\Delta_{fus}S_\mu$ of pure metals span a relatively large range, from In and Pb where $\Delta_{fus}S_\mu < R$, to Bi in which $\Delta_{fus}S_\mu \sim 2.5R$, to Sn which takes an intermediate value, where R is the ideal gas constant. Alloys and eutectics of these components cover a similar broad range, indicative of fractional contributions of different pure elemental and intermetallic phases. Relative to different monatomic solids, $\Delta_{fus}S_\mu$ in the Sn-Pb-Bi and In-Sn-Bi systems are bounded by simple metals (face-centered cubic, hexagonal closest packing, and body-centered cubic structures) on the low end and semimetals (Ge, As, Sb, Te, etc.) on the upper end (Fig. 2). Melting in In (face-centered tetragonal) and Pb (face-centered cubic) consists of an increase in configurational entropy in the system, as well as a small volume expansion. The observed $\Delta_{fus}S_\mu$ for In and Pb is consistent with $\Delta_{fus}S_\mu$ observed in transition and noble metals, albeit at significantly lower melting temperatures.[3–5] In contrast, melting in semiconductors and semimetals includes an increase in electronic degrees of freedom from tightly bound covalent solids with localized electrons to highly delocalized electrically conductive liquids, consistent with the behavior in Bi.[11,12] Electronic contributions in these cases can represent a relatively large component of the overall $\Delta_{fus}S_\mu$. In addition, well-known ideal and non-ideal mixing contributions (in both solids and liquids) may also contribute to $\Delta_{fus}S_\mu$ in eutectic alloys. Relative contributions of mixing and electronic entropy effects are detangled in the discussion.

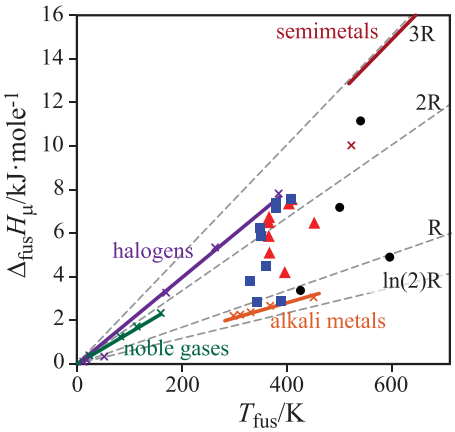

FIG. 2. Molar enthalpy of fusion of low melting point metals and alloys. Pure metals are illustrated with black circles, Sn-Pb-Bi alloys with red triangles, and In-Sn-Bi alloys with blue squares. Data for monatomic semimetals, alkali metals, noble gases, as well as diatomic halogens (reported as per mole of molecules) are included for Refs. 71 and 73. Dashed lines represent constant molar entropies of fusion, with values of some factor times the ideal gas constant, R.

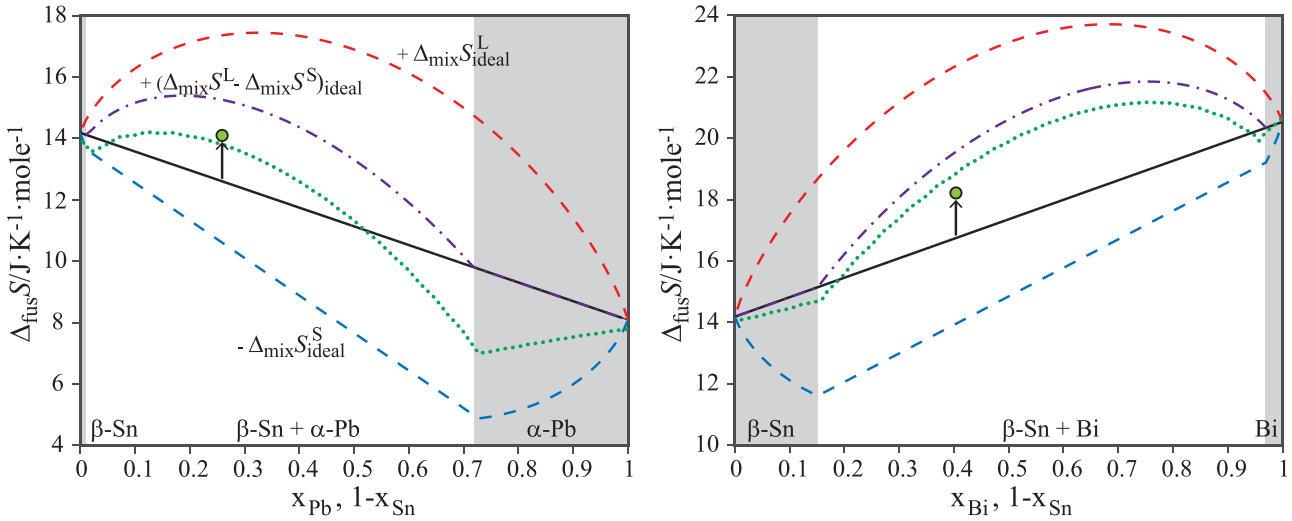

FIG. 3. Contribution of ideal and non-ideal contributions to mixing in (a) Pb-Sn and (b) Bi-Sn binaries, with mole fraction of components, x. Black line indicates linear combination of entropy of fusion of two pure metal end-members, $\sum x_i \Delta_{fus}S_i$, which holds if no mixing occurs in the solid or liquid. Dashed lines incorporate the ideal mixing contributions in the liquid phase (red) and solid phase or phases (blue). Contribution of ideal mixing in the two phase region is given by weighted molar contributions from each solid phase; single phase regions are shaded grey. Dashed-dotted line (purple) combines the effects of ideal mixing in the liquid and solid phases. Dotted line (green) incorporates non-ideal mixing terms from both solid and liquid phases, as given by Thermocalc Software TC Binary Solutions database v1.1, calculated at T_{eu}. Circle illustrates observed $\Delta_{fus}S$ for binary eutectics. Black arrows indicate the net contribution of $\Delta_{mix}S$ to $\Delta_{fus}S$ in each system.

V. DISCUSSION

A. Relative contributions from Δ_{mix}S and Δ_{elec}S

As has been previously described, $\Delta_{mix}S$ could significantly increase $\Delta_{fus}S$ in eutectics, theoretically by up to (Rln2) to (Rln3) in equiatomic binary or ternary eutectic systems, respectively. However, in real systems, solid solutions in solid phases and non-ideal entropy of mixing terms could significantly impact this contribution. It is instructive to consider two exemplar binary eutectics, Pb-Sn and Bi-Sn, where relative mixing components can be computed directly from available thermodynamic data (Fig. 3).

In both Pb-Sn and Bi-Sn, there is significant solid solution in at least one of the phases at the melting point of the eutectic, T_{eu} (α-Pb contains up to ~0.27 x_{Sn}, while β-Sn contains up to ~0.15 x_{Bi}). Thus, the net contribution of $\Delta_{mix}S_{ideal}$ to $\Delta_{fus}S$ of eutectic solids, $(\Delta_{mix}S^{L} - \sum_{\phi} x^{\phi}\Delta_{mix}S^{\phi})$ is reduced from its maximum potential value for a binary eutectic (Rln2) by a factor of ~0.5 in both Pb-Sn and Bi-Sn systems (Fig. 3).

Non-ideal entropy terms, primarily associated with $S^{E,\phi}$, act to significantly decrease the net contribution of $\Delta_{mix}S$ to $\Delta_{fus}S$ for the Pb-Sn eutectic, and to a lesser degree for the Bi-Sn eutectic (Fig. 3). Combining expressions 5 and 7, we have

$$\Delta_{fus}S = \left(S^{L} + \left(\Delta_{mix}S_{ideal} + S^{E}\right)^{L}\right) - \sum_{\phi} x^{\phi}\left(S^{\phi} + \left(\Delta_{mix}S_{ideal} + S^{E}\right)^{\phi}\right). \quad (11)$$

Thus, either negative $S^{E,L}$ or positive $S^{E,\phi}$ could reduce the contribution of $\Delta_{mix}S$ to $\Delta_{fus}S$ of eutectic solids. In the case of the Pb-Sn system, the liquid phase has a significant negative S^{E} signifying some residual degree of order in the liquid, and reducing the contribution of $\Delta_{mix}S$ to $\Delta_{fus}S$.[61] In the case of the Bi-Sn system, the net effect of non-ideal $\Delta_{mix}S$ is smaller, suggesting closer to ideal behavior in both liquid and solid phases. Thus, the net contribution of S^{E} to $\Delta_{fus}S$ of eutectic solids is reduced again by a factor of ~0.5 in Pb-Sn, but only negligibly for the Bi-Sn systems (Fig. 3). In both cases, observed data lie in reasonably good agreement with data predicted by mature thermodynamic databases.

In Pb-Sn and Bi-Sn eutectics, the effects of mixing in solid phases, as well as S^{E} terms, decreased the contribution of $\Delta_{mix}S$ to $\Delta_{fus}S$ below the ideal mixing case to only 0.20R or 0.25R, respectively. In principle, these effects could result in a negative net contribution of $\Delta_{mix}S$ to $\Delta_{fus}S$. Thus, in contrast with the originally posed theory, *it cannot be assumed that melting of eutectics will always increase* $\Delta_{fus}S$ *in a system.*[10] Considering all of the binary eutectics in the Sn-Pb-Bi and In-Sn-Bi systems, and comparing $\Delta_{fus}S$ of the eutectic against the weighted $\Delta_{fus}S$ calculated from the two end-members, it is apparent that net contributions of $\Delta_{mix}S$ to $\Delta_{fus}S$ are not always positive (Fig. 4). Importantly, this calculation neglects any mixing in intermetallic phases or different $\Delta_{elec}S$ for intermetallic phases; intermetallic phases are present in all cases where the net contribution of $\Delta_{mix}S < 0$ (Fig. 4). However, $\Delta_{fus}S$ for intermetallics are not generally available, as in many cases, these phases undergo peritectic reactions, rather than melting congruently.

The Sn-Pb and Sn-Bi binaries (Fig. 3) illustrate two examples where the net increase in $\Delta_{fus}S$ of the binary eutectic attributable to mixing effects (~1 to 2 J·K^{-1}·mol^{-1}) is significantly less than the difference in $\Delta_{fus}S$ of the monatomic endmembers (~6 J·K^{-1}·mol^{-1}), attributable to greater electronic effects in one end member over another. Other binaries investigated in this study (Fig. 4) show similar results, suggesting that electronic effects remain the dominant term influencing $\Delta_{fus}S$ in those eutectics considered here. That is, even in those cases where mixing terms introduce positive net effects to the melting of a eutectic solid,

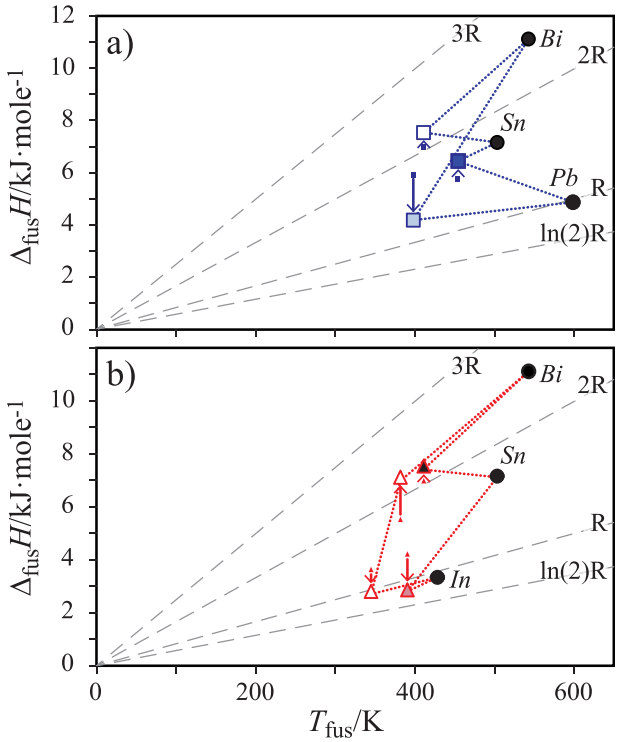

FIG. 4. Enthalpy of fusion in metals and binary eutectics in (a) Sn-Pb-Bi and (b) In-Sn-Bi alloy systems. Dashed grey lines represent points of a constant entropy of fusion (as labelled).

the increase in magnitude of $\Delta_{fus}S$ does not approach the magnitude of effects induced by including semiconducting phases with significant $\Delta_{elec}S$ contributions.

B. Consideration of binary intermetallic phases

To this point, we have largely ignored the role of intermetallic compounds. However, these compounds can simultaneously introduce both mixing and electronic contributions to $\Delta_{fus}S$. Intermetallic compounds are ordered multi-component phases, which disorder upon melting, resulting in atomically-mixed multi-component liquids. For a perfectly ordered A_xB_y compound, $\Delta_{mix}S^{\phi}$ is ideally zero (there are zero degrees of freedom in the ordered system). The entropy of fusion of that compound is therefore given by

$$\Delta_{fus}S = (S^{L} - S^{\phi}) + \Delta_{mix}S^{L}. \quad (12)$$

Thus, melting of intermetallic compounds also has the potential to increase $\Delta_{fus}S$ of a substance due to mixing effects, which is maximized at near equi-atomic compositions. In addition to mixing effects, many A_xB_y compounds composed of post-transition metals, and metalloids represent well-known semiconductor compounds in the solid phase (e.g., III-V and II-VI semiconductors), many of which melt to conductive liquids, introducing significant $\Delta_{elec}S$.

Unfortunately, intermetallic semiconductors tend to melt at very high temperatures, and therefore are not practical for many TM applications. In contrast, eutectic melting results in a depressed melting point, while still contributing some portion of the larger $\Delta_{fus}S$ of the intermetallic phase. To demonstrate this feature, we consider melting of eutectics in binary X-Sb systems (X = Al, Zn, Ga; Fig. 5). In all cases, the eutectic solid is composed of an Sb-rich phase (rhombohedral, A7 structure), as well as a stoichiometric XSb intermetallic phase. Intermetallic XSb phases are all semiconductors (ZnSb, indirect band gap 0.5 eV; GaSb direct band gap 0.70 eV; AlSb indirect band gap 1.63 eV),[62,63] suggesting that $\Delta_{elec}S$ likely plays a large role in the high $\Delta_{fus}S$ of these compounds. Furthermore, X-Sb eutectics, despite melting at lower temperatures than pure Sb, all exhibit significantly enhanced $\Delta_{fus}S$ due to combined effect of mixing and electronic contributions (Fig. 5).

C. Predicted behavior of binary eutectics in semimetals

Mature thermodynamic databases provide further insights into the contributions of electronic and mixing entropy (Figs. 6 and 7).[48] Here, we consider all known eutectics among binaries of a subset of post-transition metals and metalloids, including Al, Zn, Ga, Ge, As, In, Sn, Sb, Pb, and Bi. For the purpose of clarity, these eutectics are subdivided into those systems which do not contain intermetallic phases, and those that do. The former group illustrates the role of mixing in these systems, while the latter group is complicated by the potentially large (and in some cases unknown) $\Delta_{fus}S$ of the intermetallic phases. In line with the underlying thesis of this work, numerous eutectics are identified which exhibit both depressed T_{fus}, and increased $\Delta_{fus}S$, relative to elemental endmembers.

As before, the net contribution of $\Delta_{mix}S$ is illustrated by calculating the difference between the observed entropy of fusion, and the linear combination of $\Delta_{fus}S$ of elemental

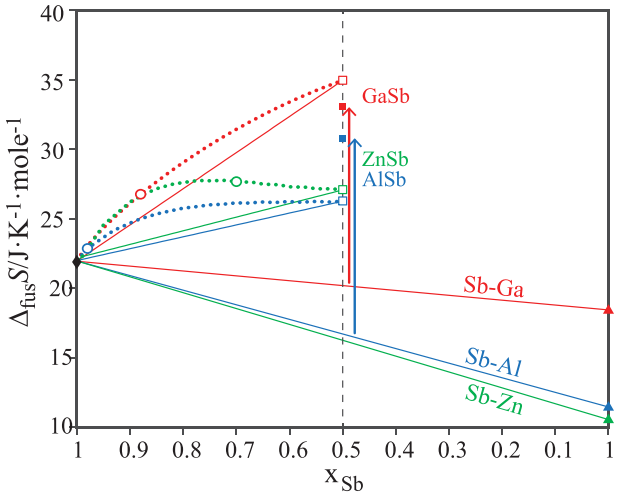

FIG. 5. Entropy of fusion of elemental Sb (diamond), XSb intermetallic phases (squares), elemental X phases (triangles), and eutectics (circles) consisting of rhombohedral Sb (A7) and XSb intermetallic phases, for X = Ga, Zn, and Al. Solid symbols represent experimentally attained data.[74] Empty symbols and dotted lines represent entropy difference between solid and liquid phases, as given by Thermocalc Software TC Binary Solutions database v1.1, calculated at T_{eu}. Thus, circles represent the entropy of fusion of the eutectics. Solid lines are guides to the eye connecting pure elemental and intermetallic phases in the same binary system. Arrows illustrate the net increase in $\Delta_{fus}S$ due to both mixing and electronic terms for the intermetallic XSb phases. ZnSb does not melt stoichiometrically, and therefore cannot be measured experimentally.

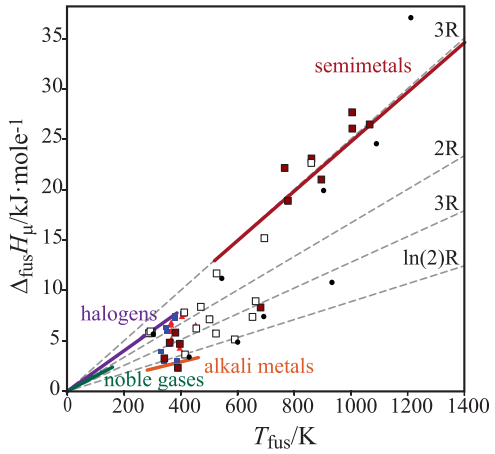

FIG. 6. Molar enthalpy of fusion predicted for binary eutectics in group IIB to V post-transition metals and metalloids including Al, Zn, Ga, Ge, As, In, Sn, Sb, Pb, and Bi. Empty squares illustrate eutectics in systems with no intermetallic compounds, while filled squares represent those eutectics which contain at least one intermetallic phase. Enthalpy of fusion of elements (black filled circles), as well as data presented in this study (see Fig. 2 for symbols), is included for reference.

endmembers: $(\Delta_{fus}S_{eu} - \sum x_i\Delta_{fus}S_i)/R$ (Fig. 3). Those systems which do not contain any intermetallic phases largely follow the regular solution mixing model [Eq. (7)]. Some cases (e.g., pts. 1–4; Fig. 7) fall significantly below the regular solution model due to non-ideal mixing effects. As has already been demonstrated for Sn_{BCT}/Bi_{Rhomb}, and Sn_{BCT}/Pb_{FCC} (Fig. 3), this negative deviation is due largely to a residual degree of order in the liquid, resulting in a significant negative S^E. Importantly, while this mechanism serves to decrease $\Delta_{fus}S$ relative to the regular solution model, there is no opposite mechanism which allows the system to exceed this model. Thus, in these systems, it is reasonable to consider the regular solution model an upper bound on the contribution of mixing entropy.

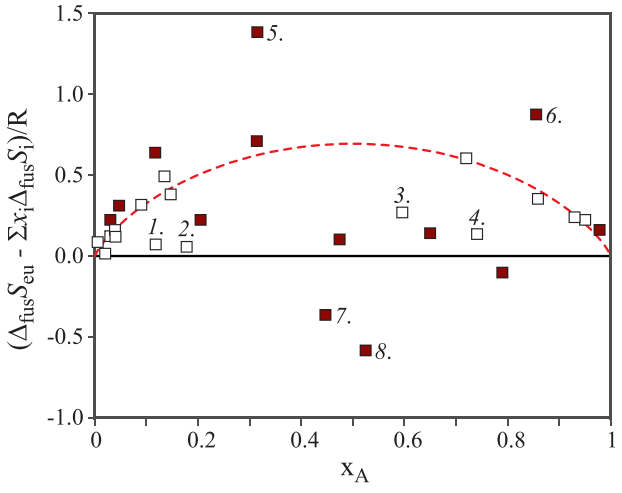

FIG. 7. Difference between $\Delta_{fus}S_{eu}$, as calculated by Thermocalc Software TC Binary Solutions database v1.1, and the weighted combination of elemental endmembers $\sum x_i\Delta_{fus}S_i$, for binary eutectics illustrated in Fig. 6. Red dashed line illustrates the ideal mixing contribution, $-R\sum_i x_i \ln x_i$. Empty squares illustrate eutectics in systems with no intermetallic compounds, including: (1) Al_{FCC}/Zn_{HCP}, (2) Pb_{FCC}/Sb_{Rhomb}, (3) Sn_{BCT}/Bi_{Rhomb}, and (4) Sn_{BCT}/Pb_{FCC}. Filled squares represent those eutectics which contain at least one intermetallic phase, including (5) $Sb_{Rhomb}/InSb_{zinc\ blende}$, (6) $As_{Rhomb}/InAs_{zinc\ blende}$, (7) $Bi_{Rhomb}/\varepsilon Pb_{HCP}$, and (8) βInSn/γInSn.

In contrast, those systems which contain one or more intermetallic phases are relatively scattered with respect to the regular solution model (Fig. 7). This results from the fact that at least one of the phases melting at the eutectic is not accounted for in the baseline (which is the linear combination of $\Delta_{fus}S$ of elemental endmembers). As examples, the eutectics at pts. 5 and 6 (Fig. 7) include a semiconducting InSb ($E_g \sim 0.25$ eV) or InAs ($E_g \sim 0.3$ eV) phase, rather than the metallic In phase, leading to a correspondingly greater $\Delta_{fus}S$ of the eutectic due to the contribution of $\Delta_{elec}S$. In other cases, such as pts. 7 and 8 (Fig. 7), solid solution in the phases present at the eutectic point negate much of the positive contribution of $\Delta_{mix}S$ to $\Delta_{fus}S$.

VI. CONCLUSIONS

1. In the case of eutectics, $\Delta_{mix}S$ can add significant contributions to $\Delta_{fus}S$, thereby affording one potential vector for design of materials with larger $\Delta_{fus}H$. However, these contributions can be strongly impacted by (1) mixing in solid solution phases, and (2) excess (non-ideal) entropy of mixing terms, suggesting that *neither of these terms can be ignored* in the general case. In the binary and ternary cases considered in this work, $\Delta_{mix}S$ was limited to a small fraction of R, the ideal gas constant.
2. In the case of semiconductors and semimetals, $\Delta_{elec}S$ contributions can easily exceed configurational and volumetric contributions to $\Delta_{fus}S$ (which occur in melting of all simple substances) contributing $\sim 2R$ to $\Delta_{fus}S$. In the Pb-Sn and Bi-Sn binaries considered, this is clearly visible as the $\Delta_{fus}S$ of monatomic Sn and Bi greatly exceed that of Pb, which is more representative of a typical metal. This trend is also observed in ternary eutectic materials which contain significant components of Bi and β-Sn phases.
3. The general conclusion for design of metallic PCMs with intrinsically high thermal conductivities and large $\Delta_{fus}H$ is to emphasize the role of phases with large $\Delta_{elec}S$ and, to a secondary extent, consider contributions of $\Delta_{mix}S$ through melting of eutectic solids whenever possible. This approach may prove especially fruitful considering melting of intermetallic semi-metal compounds, or melting of eutectics containing these phases, some of which may include significant $\Delta_{elec}S$ contributions, and the majority of which have not yet been explored in detail.

ACKNOWLEDGMENTS

The authors would like to thank Dr. D. Dudis for insightful discussions on the role of entropy in thermal storage, as well as the College of Engineering at Texas A&M University for funding to support this work.

[1]S. M. Stishov, Sov. Phys. Usp. **31**, 52 (1988).
[2]S. M. Stishov, Sov. Phys. Usp. **17**, 625 (1975).
[3]W. G. Hoover and F. H. Ree, J. Chem. Phys. **49**, 3609 (1968).
[4]J. L. Tallon, Phys. Lett. A **76**, 139 (1980).
[5]Z. Akdeniz and M. Tosi, Proc. R. Soc. London, Ser. A **437**, 85 (1992).

[6]J. Wei, Ind. Eng. Chem. Res. **38**, 5019 (1999).
[7]A. Rubčić and J. Baturić-Rubčić, Phys. Lett. A **72**, 27 (1979).
[8]A. E. Tonelli, J. Chem. Phys. **52**, 4749 (1970).
[9]R. Aranow, L. Witten, and D. H. Andrews, J. Phys. Chem. **62**, 812 (1958).
[10]C. E. Birchenall and A. F. Riechman, Metall. Trans. A **11**, 1415 (1980).
[11]B. Chakraverty, J. Phys. Chem. Solids **30**, 454 (1969).
[12]J. Van Vechten, Phys. Rev. B **7**, 1479 (1973).
[13]J. T. Economou, P. W. Wheeler, J. C. Clare, A. Trentin, S. Bozhko, T. Smith, C. Bingham, P. Stewart, R. Allarton, and J. Stewart, Proc. Inst. Mech. Eng., Part G **227**, 577 (2013).
[14]C. Chan, Proc. IEEE **90**, 247 (2002).
[15]N. R. Jankowski and F. P. McCluskey, Appl. Energy **113**, 1525 (2014).
[16]H. Mehling and L. F. Cabeza, *Heat and Cold Storage with PCM* (Springer, Berlin, 2008).
[17]A. Raghavan, L. Emurian, L. Shao, M. Papaefthymiou, K. P. Pipe, T. F. Wenisch, and M. M. Martin, in *ASPLOS '13* (2013), Vol. 41, p. 155.
[18]A. Raghavan, Y. Luo, A. Chandawalla, M. Papaefthymiou, K. P. Pipe, T. F. Wenisch, and M. M. Martin, IEEE Micro **33**, 8 (2013).
[19]L. Shao, A. Raghavan, L. Emurian, M. C. Papaefthymiou, T. F. Wenisch, M. M. Martin, and K. P. Pipe, in 2014 Semiconductor Thermal Measurement and Management Symposium (SEMI-THERM) (2014), p. 29.
[20]P. J. Shamberger, J. Heat Transfer **138**, 024502 (2015).
[21]T. Lu, Int. J. Heat Mass Transfer **43**, 2245 (2000).
[22]R. D. Weinstein, T. C. Kopec, A. S. Fleischer, E. D'Addio, and C. A. Bessel, J. Heat Transfer **130**, 042405 (2008).
[23]O. Mesalhy, K. Lafdi, A. Elgafy, and K. Bowman, Energy Convers. Manage. **46**, 847 (2005).
[24]X. Hu and S. S. Patnaik, Int. J. Heat Mass Transfer **68**, 677 (2014).
[25]H. Ge, H. Li, S. Mei, and J. Liu, Renewable Sustainable Energy Rev. **21**, 331 (2013).
[26]Y. Fukuoka and M. Ishizuka, Jpn. J. Appl. Phys., Part 1 **30**, 1313 (1991).
[27]S. Krishnan, S. V. Garimella, and S. S. Kang, IEEE Trans. Compon. Packag. Technol. **28**, 281 (2005).
[28]D.-W. Yoo and Y. K. Joshi, IEEE Trans. Device Mater. Reliab. **4**, 641 (2004).
[29]A. Evans, M. He, J. Hutchinson, and M. Shaw, J. Electron. Packag. **123**, 211 (2001).
[30]L. Shao, A. Raghavan, G.-H. Kim, L. Emurian, J. Rosen, M. C. Papaefthymiou, T. F. Wenisch, M. M. Martin, and K. P. Pipe, Int. J. Heat Mass Transfer **101**, 764 (2016).
[31]"Solder Alloy Directory," Report No. 97720 (A4) R3 (Indium Corporation, Clinton, NY, 2008), p. 15.
[32]I. Ohnuma, Y. Cui, X. Liu, Y. Inohana, S. Ishihara, H. Ohtani, R. Kainuma, and K. Ishida, J. Electron. Mater. **29**, 1113 (2000).
[33]K. Osamura, Bull. Alloy Phase Diag. **9**, 274 (1988).
[34]D. G. Archer and S. Rudtsch, J. Chem. Eng. Data **48**, 1157 (2003).
[35]D. G. Archer, J. Chem. Eng. Data **49**, 1364 (2004).
[36]S. Stølen and F. Grønvold, Thermochim. Acta **327**, 1 (1999).
[37]P. Cucka and C. Barrett, Acta Crystallogr. **15**, 865 (1962).
[38]N. Gokcen, J. Phase Equilib. **13**, 21 (1992).
[39]S. V. Stankus and R. A. Khairulin, High Temp. **44**, 389 (2006).
[40]M. Wołcyrz, R. Kubiak, and S. Maciejewski, Phys. Status Solidi B **107**, 245 (1981).
[41]R. Kubiak and K. Lukaszewicz, Bull. Acad. Pol., Ser. Sci. Chim. **22**, 281 (1974).
[42]P. Currie, T. Finlayson, and T. Smith, J. Less Common Met. **62**, 13 (1978).
[43]G. H. Otto, J. Less Common Met. **45**, 163 (1976).
[44]R. Kubiak, Z. Anorg. Allg. Chem. **431**, 261 (1977).
[45]B. B. Alchagirov, A. G. Mozgovoi, and A. Khatsukov, High Temp. **42**, 1003 (2004).
[46]B. B. Alchagirov and A. M. Chochaeva, High Temp. **38**, 44 (2000).
[47]V. Sobolev, "Database of thermophysical properties of liquid metal coolants for GEN-IV," Report No. SCK•CEN-BLG-1069 (Belgian Nuclear Research Centre, Boeretang, Belgium, 2011).
[48]J.-O. Andersson, T. Helander, L. Höglund, P. Shi, and B. Sundman, CALPHAD **26**, 273 (2002).
[49]L. Kaufman and H. Bernstein, *Computer Calculation of Phase Diagrams. With Special Reference to Refractory Metals* (Academic Press, Inc., New York, 1970), Vol. 4.
[50]O. Redlich and A. Kister, Ind. Eng. Chem. **40**, 345 (1948).
[51]A. T. Dinsdale, CALPHAD **15**, 317 (1991).
[52]A. Meyer, M. Stott, and W. Young, Philos. Mag. **33**, 381 (1976).
[53]S. Khanna, F. Cyrot-Lackmann, and P. Hicter, J. Chem. Phys. **73**, 4636 (1980).
[54]F. Pintchovski, W. Glaunsinger, and A. Navrotsky, J. Phys. Chem. Solids **39**, 941 (1978).
[55]A. Zylbersztejn and N. F. Mott, Phys. Rev. B **11**, 4383 (1975).
[56]J. D. Budai, J. Hong, M. E. Manley, E. D. Specht, C. W. Li, J. Z. Tischler, D. L. Abernathy, A. H. Said, B. M. Leu, and L. A. Boatner, Nature **515**, 535 (2014).
[57]J. W. Elmer, E. D. Specht, and M. Kumar, J. Electron. Mater. **39**, 273 (2010).
[58]L. Li, B. Zhao, B. Yang, Q. Zhang, Q. Zhai, and Y. Gao, J. Mater. Res. **30**, 242 (2015).
[59]P. J. Shamberger and T. Reid, J. Chem. Eng. Data **57**, 1404 (2012).
[60]P. J. Shamberger and T. Reid, J. Chem. Eng. Data **58**, 294 (2013).
[61]I. Karakaya and W. Thompson, J. Phase Equilib. **9**, 144 (1988).
[62]D. Benson, O. F. Sankey, and U. Häussermann, Phys. Rev. B **84**, 125211 (2011).
[63]M. O. Manasreh, *Antimonide-Related Strained-Layer Heterostructures* (CRC Press, 1997), Vol. 3.
[64]H. Kabassis, J. Rutter, and W. Winegard, Mater. Sci. Technol. **2**, 985 (1986).
[65]H. Preston-Thomas, Metrologia **27**, 3 (1990).
[66]V. Sobolev, J. Nucl. Mater. **362**, 235 (2007).
[67]H. Okamoto, in *Binary Alloy Phase Diagrams; Vol. 1*, 2 ed., edited by T. B. Massalski, H. Okamoto, P. R. Subramanian, and L. Kacprzak (ASM International, Metals Park, OH, 1990), p. 748.
[68]A. Lipchitz, G. Harvel, and T. Sunagawa, Appl. Mech. Mater. **420**, 185 (2013).
[69]V. Witusiewicz, U. Hecht, B. Böttger, and S. Rex, J. Alloys Compd. **428**, 115 (2007).
[70]E. Lemmon, M. McLinden, and D. Friend, see http://webbook.nist.gov/chemistry/ for "NIST chemistry webbook, Thermophysical properties of fluid systems," Standard Reference Database No. 69 (last accessed February 4, 2017).
[71]D. R. Lide, *CRC Handbook of Chemistry and Physics*, 90th ed. (CRC Press, Boca Raton, FL, 2010).
[72]W. R. Humphries and E. I. Griggs, *A Design Handbook for Phase Change Thermal Control and Energy Storage Devices* (NASA, Huntsville, AL, 1977).
[73]M. Chase, *NIST-JANAF Thermochemical Tables, J. Phys. Chem. Ref. Data Monograph No. 9* (American Institute of Physics, 1998).
[74]G. Stringfellow, J. Phys. Chem. Solids **33**, 665 (1972).